Effect of conservation treatments on heritage stone. Characterisation of decay processes in a case study.

M.J. Varas-Muriel [a,b,] *, E.M. Pérez-Monserrat [a,], C. Vázquez-Calvo [a], R. Fort [a]

[a] Instituto de Geociencias IGEO (CSIC, UCM), C/José Antonio Novais 12, 28040, Madrid, Spain.

[b] Facultad Ciencias Geológicas, Universidad Complutense de Madrid (UCM), C/José Antonio Novais 12, 28040, Madrid, Spain.

*E-mail address: mjvaras@geo.ucm.es

Tf- +34913944918, Fax- +34915442535

ABSTRACT

Preliminary studies are an imperative when determining the impact of conservation treatments on historical materials. The Romanesque apse on a church at Talamanca de Jarama, Madrid, Spain, whose dolostone was severely decayed by rainwater and salts, was treated in the past with substances that ravaged the restored area. Petrological techniques showed that salts leached out of the cement under the roof onto the stone cornice whose surface had been coated with synthetic resins. During evaporation, the salts precipitated in the stone and underneath the resin, inducing blistering, fissuring, flaking, scaling and detachment of part of the restored decorative elements.

Keywords: dolostone, conservation treatments, cements, synthetic resins, architectural heritage, decay, petrological techniques.

1. INTRODUCTION

Time and weathering (water, wind, solar radiation, temperature variations, air pollution...) are the chief agents of decay in most stone materials comprising the built heritage. The impact of such decay varies depending on the composition and texture of the materials involved [1-3].

The need to conserve the cultural heritage has driven the appearance on the market of many restoration products, designed and manufactured primarily to retard stone decay and increase its durability [4-7]. These products may be: inorganic (such as "lime wash" - $Ca(OH)_2$ (aq) used in the nineteenth century and presently recovered in the form of nanolime - $Ca(OH)_2$ alcoholic colloidal nanoparticles [8]) or organic, which may in turn be divided into natural (scantly processed animal or plant substances) or synthetic (primarily highly processed petroleum derivatives) compounds. A third group of products, organosiliceous derivatives such as ethyl silicates or alcoxysilanes, combines organic and inorganic compounds. All three groups are designed to: a) consolidate the internal components of the stone (consolidants); b) waterproof surfaces (water repellents); or c) rendering surfaces or fill in joints, cracks, fissures, or gaps in the stone itself (restoration mortars).

Further to international recommendations, the use of such restoration products should be limited and controlled, and only applied if they are clearly beneficial, their long-term efficacy is proven and they entail no risk whatsoever for people or the environment [9-11].

Synthetic resin and cement restoration mortars have been used profusely in recent years, for they bond well to the substrate and are highly weatherproof [4-7, 12-15]. Nonetheless, several ICOMOS Charters [9-11]) advise against using such restoration mortars in any form unless a detailed study has been conducted of their long-term performance and durability. The rationale for such recommendations may lie in these compounds' possible failure to meet the aims for which they were initially designed (render, infill, restitution of lost material,…): when combined with other construction materials they may respond in unintended ways, even generating undesirable by-products such as salts. The composition of synthetic restoration mortar varies depending on its intended purpose and the construction materials with which it is to be in contact. As a general rule, such mortars comprise a binder (cement, lime/hydraulic lime or gypsum), siliceous or carbonaceous sand aggregate, pigments for colour and admixtures such as polymeric resins, silicone or siloxane resins, acrylic resins, epoxy resins, fluorinated polymers or unsaturated polyesters [12, 14-15].

Like decay itself, conservation and restoration products perform differently depending on the type of stone to which they are applied and on environmental conditions. Hence the need for preliminary studies [6, 12, 16-18], firstly to characterise the composition and texture of the stone substrate. In particular its porosity must be determined (pore percentage, shape, size and distribution) and its condition assessed (forms, causes, processes and agents of decay), paying close heed to local environmental factors or microclimatic conditions inside the building to be conserved [6-7, 12, 19-20]. That should be followed by a field or/and laboratory study of the restoration products and application techniques to establish their efficacy, their compatibility with and suitability for the stone substrate, and their durability in the prevailing climate [1, 7, 12-14, 16-17, 20].

While preliminary studies are called for in international recommendations and protocols for action on world cultural heritage conservation (e.g., Athens 1931, Venice 1964, Restauro 1987 Charters, to name a few; ICOMOS), they are often absent in restoration project design and implementation. The distressing result has been that many interventions in heritage buildings have accelerated decay in the materials they set out to protect [1, 12, 14, 17, 21].

Moreover, since the full chemical formulation of market products is normally unknown, preliminary trials provide information from which to more or less accurately predict their possible long-term behaviour [7, 16-18, 21-23]. This is of particular relevance because the original chemical composition of these products may vary with time, depending on their interaction with the material to be restored and the local environment, and may become irreversible for disposal. In a similar vein, gaining a subsequent understanding of the product applied and the application technique used may be a complex task if no documentary record of the intervention is available [12, 14, 17].

1.1. San Juan Bautista Church at Talamanca de Jarama, Madrid, Spain: apse construction and restoration

San Juan Bautista Church is located at Talamanca de Jarama, a village 45 km NNE of Madrid, Spain. Characterised by two architectural styles, Romanesque (twelfth-thirteenth centuries) and Renaissance (sixteenth century), the church is made of dolostone, limestone and quartzite ashlars and rubble stones; brick masonry; earthen infills; and mortars, both as jointing and as renser. The rectangular presbytery and semi-circular apse (Fig. 1) are all that is left of the original Romanesque dolostone building. The rectangular nave or main body of the church, consisting of three aisles with varying heights, was rebuilt in Renaissance style in the sixteenth century with a wide variety of construction materials (stone, brick and mortars). In 1885, with the church in ruins, the south wall and bell tower were rebuilt. The building was listed as a historic-artistic monument in 1931 and has been protected as such ever since.

The semi-circular apse was built around four pilasters that delimit five walls or infills. Its three windows are located in alternate infills (Fig. 1). The stone masonry consists of rough ashlars at the base and more refined ashlars in the upper areas. The floral, geometric and human forms carved out of the stone modillions and cornice, are of significant historic and artistic value (Figs 2 and 3). The dolostone on the apse, traditionally used in the area, was quarried from nearby Upper Cretaceous geological formations [24].

The two types of dolostone were quarried from different geological strata. One, beige-coloured, compact and scantly porous, is found in the rough ashlars at the base, while the other, a yellowish and more porous stone, is found in the upper walls ashlars, including the decoratively carved modillions and cornice (Figs 1 and 2). The former is known as *Piedra de Torrelaguna* (*Torrrelaguna stone*) and the latter and more workable, *Piedra de Redueña* (*Redueña stone*) [2]. Some of the stone in the dado and underneath the modillions was replaced (possibly in the 1885 intervention) with the same varieties of dolostone as the original material. The lighter tone cladding visible in the same areas was laid during the 1990 restoration (Fig. 1).

In the late nineteen seventies, the apse was observed to be largely decayed, due primarily to the damp accumulating in the dado, cornice and windows, attributed respectively to capillary moisture rising from the subsoil, rainwater leakage and surface runoff. The main causes of decay in the cornice were the poor condition of the roof and the lack of any means to evacuate rainwater. The effect of rainfall (475 mm/year) is more conspicuous in the spring and autumn. A design for intervention proposed in 1982, rather vaguely and with no mention of preliminary studies, called for "repairing the roof, chipping away the mortar-patina covering the entire apse and replacing the ashlars and other architectural elements with stone similar in appearance to the original material".

The design specified that the walls were to be cleaned with spray-dried water and scoured with ammonium bi-fluoride, after which protective treatment (Primal AC-234 acrylic resin with methyl methacrylate and ethyl acrylate co-polymers) would be applied. The joints and cracks were also to be cleaned and filled with cement or/and (Araldite BY-154) epoxy resin and (AFA 55/60) siliceous sand. In the most damaged part of the cornice, some of the carved decorative elements had fallen away and many others were severely decayed. Restoration was to consist of the application first of a pure epoxy resin consolidant and then of (Araldite BY-154) epoxy and (Primal AC-33) acrylic resins mortars containing siliceous sand to restitute forms and textures.

The visual inspection undertaken on the occasion of the present study, in the absence of written records on whether this restoration design was implemented as envisaged or partially or fully modified, revealed that the intervention conducted in 1990 primarily affected the Romanesque apse. One of the measures adopted at the time was to replace a few ashlars with white limestone quarried outside the region that differs from the original stone (Fig. 1). The roof was weatherproofed with a grey portland cement mortar under the arabic roof tiles, that was also laid directly on the cornice (Figs 2 and 3); joints and cracks were filled in with cement and synthetic mortars (Fig. 3); and a number of conservation products were applied in an attempt to protect the decorative elements on the cornice as far as possible (Fig. 3). By 2005, the restored stone exhibited conspicuous and troubling signs of decay: the decorative elements on the cornice were severely deteriorated, with risk of detachment [25].

The present study aimed to: a) assess the state of decay in the carved stone on the Romanesque cornice prior to the 1990 intervention; b) ascertain the type of restoration products used in that intervention; c) establish the degree of interaction with and the suitability of these products for the stone and other materials; and d) define the mechanisms involved and the type of decay induced by these products. Petrological techniques, regarded as one of the first analytical methods to be deployed prior to restoration, were applied to meet these objectives. The observation, description and direct and objective classification of decay to small-scale in a material constitute a sound basis for defining the agents, causes and processes of damage and for endorsing the findings of other more complex and subjective analytical approaches.

2. MATERIALS AND METHODS

The samples studied were taken from the yellow dolostone on the upper area of the original apse, and primarily from the elements carved into the modillions and cornice. Three 5 cm diameter, 15-cm long core samples were taken from an ashlar underneath the cornice (Fig. 4a), along with fragments of varying size from the cornice itself (Fig. 4b).

Petrological, mineralogical and chemical composition were analysed with the techniques described below to characterize the cornice materials and determine its state of conservation, and theorise about the causes and mechanisms involved in the poor response of the stone to the treatments applied.

- Polarised light optical microscopy (PM) was conducted to Spanish and European standard UNE-EN 12407 [26] on an Olympus BX51 petrographic microscope fitted with an Olympus DP12 digital camera. The samples were so severely segregated that they had to be consolidated with epoxy resin prior to preparing the 3x2-cm, 30-μm thick thin sections, dyed with alizarin red [27] to differentiate calcite from dolomite. PM afforded information on the composition, texture and microstructure of the materials sampled.
- Electron microscopy (SEM-EDS) studies were performed on a JOEL JSM 6400 scanning electron microscope fitted with an Oxford-Link Pentafet energy dispersive X-ray microanalyser. Small fragments (~1.7 cm^3) and thin sections of the samples were scanned under a secondary electron (SE) beam. Both types of samples were graphite-coated with a BALZERS MED 010 deposition system, to make them conductive. SEM revealed component microstructure and texture on a smaller and more detailed scale than PM. In addition, the use of EDS in point mode furnished a semi-quantitative chemical analysis of the components.
- Crystalline minerals were identified on a PHILIPS PW 1752 X-ray diffractometer fitted with a copper anode tube and PC-ADP diffraction software. XRD patterns were acquired operating at 40 kV and 30 mA at 2θ angles of 2–65° with a 0.02-step scan, a speed of 2° per minute, CuKα radiation and a graphite monochromator. The powder fraction (particle size under 50 μm) of the total samples, were analysed.
- Solid samples were exposed to micro X-ray diffraction (μXRD) to identify certain mineral phases on a micrometric scale. The facility used was a PHILIPS X'Pert MPD diffractometer with a double goniometer, CuKα radiation and a curved Cu monochromator. Measurements were taken at 45 kV and 40 mA. μXRD patterns were acquired in the 2–65° 2θ range using a 0.02-step scan at a rate of 1° per minute.
- The chemical composition of the conservation treatments was found with Fourier transform infrared spectroscopy (FTIR) on a NICOLET Magna FTIR 750 analyser at a resolution of 0.5 cm^{-1} and a working range of 4 000-350 cm^{-1}. The samples were powdered and pressed into potassium bromide (KBr) pellets. Qualitative analysis was based on the specifications and recommendations proposed by Derrick et al. [28].
- Dolostone petrophysical characterisation and evolution were determined from density, open porosity, water absorption (UNE-EN 1936 [29]) and ultrasonic P-wave pulse velocity (Vp)

(UNE-EN 14579 [30]) findings. These physical properties were measured at normal atmospheric pressure and ambient temperature. The tests were conducted on both the outer and inner areas of the cores. The Vp values were found on a PUNDIT CNS ELECTRONICS LTS portable analyser, fitted with 54 kHz, 50-mm diameter transducers.

3. RESULTS

3.1. Cornice: state of conservation

The yellow dolostone on the cornice was found to be severely decayed and many of its decorative elements to have been totally or partially lost after the 1990 restoration (Fig. 3). Some of the conservation treatments contributed to the decay of the dolomite substrate (Fig. 5). The main forms of decay detected were: a) surface gloss and change in hue from yellow to grey in the carved stone due to the presence of a viscous film (Figs 4b and 5); b) blistering, fissuring, flaking and scaling both in the surface treatment and the carved stone, resulting on occasion in detachment (Fig. 5); c) saline sub-efflorescence and crypto-efflorescence beneath the treatments, affecting the carved stone; and d) surface wear (Figs 2, 3 and 5).

3.2. Characterisation and condition of the stone substrate

The dolostone on the cornice is a carbonate rock, uniform in appearance whose ~20-% porosity consisted of pores of < 500 μm in diameter (visual estimate; Fig. 4a). The sub-parallel cracks up to 1.5 cm deep on the surface exposed to the elements induced scaling and detachment with the concomitant loss of the figures carved in the stone (Figs 5 and 6).

The PM study revealed that this massive dolostone is characterised by rhomboid micritic dolomite crystals measuring <10 μm on average and 20-25-% intercrystalline porosity (Figs 7a and 7b).

Some of these subrounded (mean diameter = 225 μm) or irregularly shaped (mean diameter = 975 μm) pores were filled with ≥30-μm sparry calcite crystals. Disperse monocrystalline quartz grains (±5 %) with a mean size of <150 μm (very fine sand) were observed inside the dolomicritic mass (Fig. 7a). The numerous dark iron gel spots also observed were partially responsible for the yellow-golden tone of this variety of stone (Fig. 7a), classifiable as a dolomudstone [31]. The mineralogy detected under the PM (dolomite and some quartz) was confirmed by the XRD findings.

The intense cracking on the sample surfaces increased in the outward direction (Fig. 7b). These cracks, parallel and sub-parallel to one another and to the outer surface of the sample, were 75 μm thick on average and over 250 μm thick in the outer-most areas.

Further to the petrophysical findings (Table 1) this is a dense (>2 800-kg m^{-3}) but highly open porosity (24-26 %) stone, properties that were observed to vary from the outer-most decayed

(0-5 cm) to the inner (5-10 cm) intact inner area of the cores. The porosity in the outer stone was up to 8 % higher than in the inner stone, which translated into 10 % greater water sorptivity. Such higher surface porosity was confirmed by the nearly 1 000-$m \cdot s^{-1}$ lower ultrasonic P-wave velocity (Vp) in that area than in the inner stone.

3.3. Characterisation of conservation treatments

This study detected the presence of three types of conservation treatments.

A- The cornice has a 1 to 8-mm thick grey mortar rendering containing white particles that adapts to the surface irregularities in the intensely cracked stone substrate (Fig. 6). This mortar bonded apparently well to the stone, although not uniformly, for the non-filled millimetric pores found in some areas may have facilitated detachment (Figs 6 and 8).

From the petrological (PM) standpoint, this mortar was observed to be a dark, granular, uniform and massive mix of crypto-crystalline (crystal size <4 μm), sub-angular limestone aggregate of varying size (0.125-0.250 and 0.5-1 mm) agglutinated in a partially carbonated, light colour matrix-binder with a microcrystalline texture (crystal size <10 μm) (area A in Fig. 8a). The aggregate-binder interface was well-defined with no chemical reactions taking place around the edges. Porosity was <5 % and characterised by circular to semi-circular pores with a mean diameter of 0.5 mm. The μXRD mineralogical analysis confirmed that the aggregate was calcite and the binder calcite with some quartz (Fig. 8b).

Under SEM (area A in Fig. 8c, and Fig. 9), the mortar exhibited dark, dense, viscous areas (matrix-binder) sharply interfaced with lighter micro-granulated areas (aggregate). EDS revealed that the chemical composition of the two areas differed clearly. Despite the graphite coating on the samples, the dark binder area (point A in Fig. 9) exhibited a much higher C (organic component) concentration than the lighter aggregate area (point B in Fig. 9), which in contrast had more Ca (calcite) than the binder. Other chemical elements present in the two areas, although more prominently in the binder, included Si, Mg, Al, Na and Cl (neither Cl nor Na were found in the aggregate). A detailed study of the binder revealed the presence of small (3-5-μm) Ca (calcite) particles inside a C-high dark, dense gel with some Si.

The FTIR spectrum for this mortar (Fig. 10) contained a vibration band in the 1 740-cm^{-1} region associated with carbonyl (C=O) and an especially intense vibration band at around 1 440 cm^{-1} attributed to carbonate groups ($-CO^{=}_{3}$). The bands detected at around 714, 730, 876, 1 440, 1 800 and 2 530 cm^{-1} were attributed to calcite (CO_3Ca). The intense vibration band in the 3 430 to 3 540 cm^{-1} region as well as the absorption band at around 1 620 cm^{-1} were associated with hydroxyl (structural O-H) and amine (N-H) groups. The bands at 1 440 and 2 890 to 3 030 cm^{-1}

were attributed to the C-H group and the ones at 1020-1250 cm^{-1} with C-N and C-O groups. The weak vibration band at 1 080 cm^{-1} was associated with the presence of silicic acid (Si-O-Si).

B - This restoration mortar and at times the stone itself were found to bear a 25 to 50-µm thick coating (area A in Fig. 11a). A viscous film adapted to the surface irregularities of the substrate, it explained the surface gloss observed (Fig. 4b and area A in Fig. 11b). According to EDS analysis, its chemical composition included Ca, C (less than in the mortar) and some Si (point A in Fig. 11b).

The FTIR spectrum for the coating (Fig. 12) differed clearly from the pattern for the restoration mortar. The very intense vibration band in the 1 740 cm^{-1} region associated with a carbonyl group (C=O) predominated over the band at 1 450 cm^{-1} attributed to carbonates ($-CO^{=}_{3}$). The bands detected in the 714-, 876-, 1450- and 2 530-cm^{-1} regions were generated by calcite (CO_3Ca). The intense vibration band at around 3 430 to 3 540 cm^{-1} as well the band at 1 630 cm^{-1} were associated with hydroxyl (structural O-H) groups. The intense bands at 1 450 and 2 880 to 2 970 cm^{-1} were attributed to the C-H group and the ones at 750 to 800, 1 070, 1 160, and 1 250 to 1 270 cm^{-1} to C-O groups. Silicic acid (Si-O-Si group) appeared in the form of weak bands in the 471-, 523-, 675- and 1 070-cm^{-1} regions. C-O and C-H groups were also prominent in this film.

C - In the cracked stone substrate (areas C in Fig. 8 and D in Fig. 13), the Ca-, Mg- and Fe-bearing dolomite crystals and the inter-crystalline and fracture porosity were covered with a thin film only detectable under SEM. Its main (EDS-analysed) chemical composition included Si and Al, while C was scantly present. PM observation (Figs 7 and 8) revealed the presence of this treatment indirectly, for the fracture porosity was not filled with the salts detected.

3.4. Characterisation of saline degradation products

According to the petrographic (PM, XRD and SEM-EDS) findings, appears a new mineralogical component, micro-crystalline gypsum - $SO_4Ca{\cdot}2H_2O$ (areas B in Fig. 8 and C in Fig. 13). It was detected below the conservation surface treatments, primarily at the interface between the restoration mortar and the cracked dolostone, where it formed a massive irregular layer 0.5 to 1 mm thick (Figs 8 and 14a). It also appeared inside the cracked stone where it formed subspherical growth nodules (Figs 8 and 14) up to 300 µm in diameter, interconnected by thin capillaries (Fig. 14b). The gypsum nodules were observed at depths of up to 1.5 cm and to migrate outward to the stone surface where they formed the layer of variable thickness under the restoration mortar (Fig. 14a). No gypsum fill was found in the cracks in the stone substrate.

4. DISCUSSION

The main type of decay found in the *Piedra de Redueña* [2] dolostone forming the carved cornice on the Romanesque apse was intense inner cracking parallel to the surface, at depths of up to 1.5 cm (Figs 6 and 8). On the surface, this cracking translated into flaking and scaling liable to detachment.

The main agents of decay identified were rainwater and soluble salts due to continuous leaking and surface runoff, by the poor pre-1990 condition of the roof and the total absence of gargoyles and gutters to evacuate rainwater. Cracking, characteristic of this variety of stone when exposed to water and salts [32], was the type of decay exhibited by the dolostone in the cornice prior to the 1990 restoration [25].

This stone's high open porosity (~25 %, Table 1) makes it a readily workable and easy to carve but at the same time scantly durable material [2, 32]. For that reason, it was used on the upper areas of the apse, including the cornice, while a similar but less porous and hence more durable variety (*Piedra de Torrelaguna*, [2]) was laid in the lower areas.

The mortar covering the carved dolostone in the cornice, applied in 1990 to restitute the lost stone (Figs 6, 8, 9 and 13), appeared to be a mix of lime powder with at least two types (epoxy and acrylic) of synthetic resins and mudstone-like limestone aggregate [31] (Figs 8 and 9). The restoration design drafted in 1982 specified neither the lime (actually calcite - CO_3Ca) binder nor the limestone aggregate (Fig. 9). The synthetic resins in this mortar were identified on the grounds of the vitreous and viscous appearance of the binder under SEM-SE (Figs 9 and 13) [17-18], the EDS-detected presence of high levels of carbon (C) (Figs 9, 11 and 13) and the carbonyl group (C=O) revealed by FTIR analysis (Fig. 10) [4, 27]. Inasmuch as the resins were mixed, their chemical composition would be very difficult to ascertain with absolute certainty. One of the resins may be regarded as acrylic given the FTIR identification of C-O and C-H groups, while the presence of N-H and C-N groups in the other denotes an epoxide composition [4, 27]. The existence of the epoxy was also confirmed by the EDS detection of NaCl (point A in Fig. 9), which may have arisen during hardening [4]. Both types of resins were called for in the 1982 design. The quartz (µXRD – Fig. 8b), Si and Al (EDS - point A in Fig. 9) and Si-O-Si groups (FTIR – Fig.10) found in this restoration mortar, in turn, suggested the possible presence of a third, silica compound-based consolidant [12, 17-18] or a possible chemical change in one of the synthetic resins used. No written information was available to corroborate the presence of such a third conservation product.

The viscous, glossy film covering both the aforementioned restoration mortar and at times the dolostone itself contained both Ca and C (Figs 11 and 13). The identification of C=O, C-O and C-H groups was an indication that it may have been an acrylic resin [5, 28] mixed with lime powder (Fig. 12).

In another vein, the treatment applied prior to the restitution mortar in 1990 was designed to consolidate the decayed dolostone by sealing its cracks (Figs 8 and 13). The EDS identification of silicon (Si) and aluminium (Al) with very little carbon (C) may have been the result of the presence of a silica compound-based product [12, 17-18] similar to the substance detected in the mortar,

rather than the epoxy resin specified in the 1982 design. This product appeared (PM-SEM) to have penetrated to a suitable depth (1.5-2 cm), filling most of the cracks in the stone. Proof of such effective penetration was that the gypsum that appeared as an undesirable by-product of decay did not precipitate into these cracks (Figs 8 and 14a). Good penetration is an essential feature of consolidants used in restoration [6-7, 12, 16, 33].

The gypsum ($SO_4Ca{\cdot}2H_2O$) present in this area was generated after the 1990 restoration and appeared to be the direct cause of the accelerated decay observed in the restored cornice. It adopted the form of sub-efflorescence underneath the treatments used to restore the cornice ornaments and crypto-efflorescence inside the cracked stone (Figs 8, 13 and 14). While internal, this mineral was not attributable to the dolostone, for the salts originated during stone decay, such as epsomite or hexahydrite, are magnesium sulfate-based [34]. Rather, its origin was associated with the grey portland cement mortar laid in 1990 both underneath the apse roof tiles and directly on the carved cornice, filling joints and cracks between the ashlars comprising the cornice (Fig. 3). After 1990, dissolved sulfur and calcium salt-laden rainwater leaking through the roof generated an ionic charge in the underlying cement mortar [14, 35]. These ionic solutions seeped into the dolostone beneath the cornice and flowed fairly freely inside the highly porous stone, working their way outward to the surface during the evaporation induced by the local climate (dry and very warm summers >30 ºC [20]). The restoration treatments used to restitute and conserve the outer ornaments prevented these solutions from exiting the stone, however (Fig. 15) [25].

Prevented by the presence of silicate consolidant inside the cracks, gypsum precipitated in the pores not penetrated by the conservation product. These pores were inter-connected by capillaries running across the treatment (Figs 14b and 15). Gypsum precipitation in the pores induced the growth of sub-spherical nodules up to 300 μm in diameter and internal stress as a result of crystallisation (Figs 8 and 14). These gypsum nodules were the saline crypto-efflorescences observed inside the dolostone, and whose formation could be explained in a similar way to the formation (controlled by substrate porosity) of evaporite nodules in sebkha zones (current geological environments characterised by climatic intense evaporation) [36-37].

During saline solution migration toward the stone surface, the salts precipitated, clustering under the surface treatments (restoration mortar or surface film) that they were unable to permeate (Figs 8, 13, 14a and 15). As a result, a layer of gypsum of varying thickness appeared between the surface treatments and the cracked-consolidated stone, especially where the bond between them was weak. The continuous crystallisation-induced stress of salts destabilised the restored ornament. These sub-efflorescent clusters underneath the coating film (acrylic resin) caused swelling, fissuring, flaking and detachment in both layers. When saline sub-efflorescence was located under the (epoxy and

346 acrylic resins) restoration mortar, scaling and surface detachment prevailed. Such types of decay
347 affected the restoration mortar, the gypsum layer and even part of the cracked dolostone, with the
348 total or partial loss of the restored ornament (Fig. 5).

349 After part of the treatments and the carved stone surface fell away, the rest of the carved stone
350 substrate (ornament) was weakened by the presence of salt efflorescence, which continued to induce
351 powdering and crumbling stone. The resulting detachment entailed the disappearance of valuable
352 decorative elements on the cornice restituted in 1990 [25].

353 In 2006 the apse was the object of further intervention, in which the cement bedding mortar was
354 replaced with lime mortar in the joints and cracks in the cornice, although the cement mortar
355 underneath the roof tiles was not removed. The cantilever was also enlarged slightly to protect the
356 cornice from the sun and rain, but no alternative system was devised to prevent rainwater from
357 leaking into the cement mortar and generating salts (gypsum). The cornice and its decorative
358 elements were again treated. The salts were eliminated with cellulose poultice; the most severely
359 damaged areas were consolidated with a mix of epoxy resin, marble powder and acetone; hydraulic
360 lime mortars physically similar to the stone were used to restitute the detached elements; and the
361 entire monument was consolidated by spraying its surface with an organo-siliceous product. Decay
362 may re-appear in the area, however, inasmuch as water will continue to leak across the cement in
363 the roof and evaporate outward to the surface of the cornice. Is a decay mechanism which acts from
364 the inside to outside. That notwithstanding, in the 2006 restoration preliminary studies were
365 conducted to determine the condition of the apse and how restoration might best be broached. A
366 number of restoration products and application techniques were tested, which to date (2015) have
367 not posed any conservation problems. On that occasion, the preliminary studies and restoration
368 works, conducted in 2005 and 2006, were well documented for use as guidance in future
369 interventions.

370

371 5. CONCLUSIONS

372 - The alarming decay on the ornamental part of the upper area of the Romanesque apse to San Juan
373 Bautista Church, restored in 1990, was the result of misguided intervention design and
374 implementation, in turn due to the want of a preliminary study that would have helped identify the
375 type of stone substrate, its conservation state and possible response to certain conservation
376 treatments.

377 - The variety of stone on the ornament-bearing apse modillions and cornice was identified as a very
378 porous, scantly durable dolostone decayed by rainwater leakage and surface runoff, along with the

concomitant salts. The forms of decay observed were internal cracking, flaking, scaling and surface detachment.

- The use of cements and synthetic resins on a poorly conserved porous stone failed to meet the general standards of effectiveness, suitability and durability required of conservation and restoration treatments to ensure the physical stability of the restored area.

- Most of the ornaments restored in 1990 decayed and were lost in very short order due to the appearance of an undesirable by-product (salts) of the restoration treatments applied.

- The use of portland cement mortars on the cornice and its joints led to the presence of ionic saline solutions (gypsum) inside the dolostone.

- The silicate consolidant used to seal the cracks in the stone substrate on the cornice penetrated to a suitable depth (1.5-2 cm) but was not 100 % effective, for some pores remained connected, providing channels for the water and dissolved salts to migrate toward the surface. The salts precipitating in these pores formed nodules that constituted saline crypto-efflorescences which, while not the direct cause of decay, may have induced internal stress that weakened the surface structure of the cracked stone.

- The epoxy and acrylic resins mortar used to restitute the lost ornamental elements stiffened and hardened, obstructing the exit of the dissolved salts inside the stone. These salts precipitated between the stone and the synthetic mortar, forming a layer of gypsum of varying thickness (saline sub-efflorescence). The decay in these areas consisted primarily of scaling and possible detachment either around the gypsum layer or the cracks in the dolostone, disfiguring the restored ornament.

- The acrylic resin water repellent applied rendered the surface glossy and changed the yellowish-gold hue of the original dolostone to a greyish tone. Moreover, it blistered, fissured, flaked and became detached, detracting from the appearance and condition of the cornice.

- The use of petrological techniques such as PM and SEM revealed the processes and agents involved in the progressive decay of the Romanesque cornice restored in 1990 and the respective mechanisms.

Acknowledgements

This study was funded under project of MICCIN (CGL2011-27902) and forms part of the GEOMATERIALES-2CM (S2013/MIT-2914) research programme. The authors are members of the Complutense University of Madrid's Research Group: *''Alteración y Conservación de los Materiales Pétreos del Patrimonio"* (ref. 921349) and of the CEI-Moncloa (UCM-UPM) through RedLabPat. Thanks are owed to the Archbishopric of Alcalá de Henares, Madrid, and all the

persons associated with the church in Talamanca for their assistance throughout this study. Manuscript edited by Margaret Clark, professional translator and English language science editor.

REFERENCES

[1] Binda L, Saisi A, Tedeschi C. Compatibility of materials used for repair of masonry buildings: research and applications. In: Kourkoulis SK editor. Fracture and Failure of Natural Building Stone. Springer Netherlands; 2006, p. 167-182.

[2] Fort R, Varas MJ, Álvarez de Buergo M, Freire DM. Determination of anisotropy to enhance the durability of natural stone. Journal of Geophysics and Engineering 2011; 8: S132-S144.

[3] Guardia-Olmedo JJ, Varas-Muriel MJ, Suárez-Medina FJ. Castle-Palace of La Calahorra, Granada: Influence of climatic and architectural factors in the differential deterioration of stone masonries. Materiales de Construcción 2013; 63 (312): 597-612.

[4] Ginell WS, Coffman R. Epoxy resin-consolidated Stone: Appearance change on aging (Architectural restauration). Studies in Conservation 1998; 43 (4): 242-248.

[5] Banthia AK, Gupta AP. Role of acrylic resin in the conservation of deteriorated khondalite stones. Polymer Preprint (ACS) 2000; 41(1): 277–278.

[6] Cnudde V, Cnudde JP, Dupuis C, Jacobs PJS. X-ray micro-CT used for the localization of water repellents and consolidants inside natural building stones. Materials Characterization 2004; 53: 259–271

[7] Vacchiano CD, Incarnato L, Scarfato P, Acierno D. Conservation of tuff-stone with polymeric resins. Construction and Building Materials 2008; 22: 855–865

[8] López-Arce P, Gómez-Villalba L, Pinho L, Fernández-Valle ME, Alvarez de Buergo M. Fort R. Influence of porosity and relative humidity on consolidation of dolostone with calcium hydroxide nanoparticles: Effectiveness assessment with non destructive techniques. Materials Characterization 2010; 61: 168–184

[9] Washington 1987 Charter. Charter for the conservation of historic tows ans urban areas. ICOMOS General Assembly in Washington, DC, 1987. http://www.icomos.org/en/charters-and-texts

[10] ICOMOS 1996. Principles for the recording of monuments, groups of buildings and sites. 11th ICOMOS General Assembly in Sofia, 1996. http://www.icomos.org/en/charters-and-texts

[11] ICOMOS 2003 Charter. Principles for the analysis, conservation and structural restoration of architectural herigate. 14th ICOMOS General Assembly in Victoria Falls, Zimbabwe, 2003. http://www.icomos.org/en/charters-and-texts

444 [12] Varas MJ, Álvarez de Buergo M, Pérez-Monserrat E, Fort R. Decay of the restoration render mortar of
445 the church of San Manuel and San Benito, Madrid, Spain: Results from optical and electron
446 microscopy. Materials Characterization 2008; 59 (11): 1531-1540.

447 [13] Domingo C, Alvarez de Buergo M, Sánchez-Cortés S, Fort R, García-Ramos JV, Gómez-Heras M..
448 Possibilities of monitoring the polymerization process of silicon-based wáter repellents and consolidants
449 in stones through infrared and Raman spectroscopy. Process in Organic Coatings 2008; 63: 5-12.

450 [14] Pecchioni E, Gomez-Ubierna M, Cagnini A, Galeotti M, Fratini F, Porcinai S. Ancient and new repair
451 mortars for conservation: application to the case of San Leonardo Pulpit (Florence, Italy). International
452 Journal of Architectural Heritage 2014; 8 (4): 556-580.

453 [15] Nóvoa PJRO, Ribeiro MCS, Ferreira AJM, Marques AT. Mechanical characterization of lightweight
454 polymer mortar modified with cork granulates. Composites Science and Technology 2004; 64: 2197-
455 2205.

456 [16] Álvarez de Buergo Ballester M, Fort-González R. Basic methodology for the assessment and selection
457 of waterrepellent treatments applied on carbonatic materials. Prog Org Coat 2001; 43: 258– 266

458 [17] Varas MJ, Álvarez de Buergo M, Fort R. The influence of past protective treatments on deterioration of
459 historic stone façades: A case study. Studies in Conservation 2007; 52: 110-125

460 [18] Álvarez de Buergo M, Fort R, Gómez-Heras M. Contributions of SEM to the assessment of the
461 effectiveness of stone conservation treatments. Scannig 2004; 26 (1): 41-47.

462 [19] Van Hees RPJ, Binda L, Papayianni I, Toumbakari E. Characterisation and damage analysis of old
463 mortars. Materials and Structures 2004; 37 (273): 644-648.

464 [20] Varas-Muriel MJ, Fort R, Martínez-Garrido MI, Zornoza-Indart A, López-Arce P. Fluctuations of the
465 indoor environment in Spanish rural churches and their effects on heritage conservation: hygro-thermal
466 and CO_2 conditions monitoring. Building and Environment 2014; 82: 97-109.

467 [21] Valluzi RM, Binda L, Modena C. Experimental and analytical studies for the choice of repair techniques
468 applied to historic buildings. Materials and Structures 2002; 35 (249): 285-292.

469 [22] Ibáñez-Gómez JA, Yusta I, García-Garmilla F, Cano M, Rodríguez-Maribona I, Beraza K, Garín S.
470 Chemical and mineralogical study of restoration mortars applied to the Eocene sandstones of Gipuzkoa
471 used for building contruction. Geogaceta 2001; 30: 223-226.

472 [23] López-Arce P, Zornoza-Indart A, Gómez-Villaba LS, Fort R. Short- and Longer-Term Consolidation
473 Effects of Portlandite Ca(OH)2 Nanoparticles in Carbonate Stones. Journal of Material Civil
474 Engineering 2013; 25: 1655-1665.

475 [24] Fort R, Álvarez de Buergo M, Pérez-Monserrat E, Gómez-Heras M, Varas-Muriel MJ, Freire DM.
476 Evolution in the use of natural building stone in Madrid, Spain, Quarterly Journal of Engineering
477 Geology and Hydrogeology 2013; 46: 421-429.

[25] Vázquez-Calvo C, Varas MJ, Pérez-Monserrat E, Álvarez de Buergo M, Fort R. The causes of the accelerated stone decay by means of optical Microscopy and SEM-EDS. In: Abstract book, 11th Euroseminar on Microscopy Applied to Building Materials. Porto, Portugal, 2007: 109-110.

[26] UNE-EN 12407. Métodos de ensayo para piedra natural. Estudio Petrográfico. Asociación Española de Normalización y Certificación (AENOR), Madrid, 2007.

[27] Lindholm RC, Finkelman RB. Calcite staining: semiquantitative determination of ferrous iron. Journal of Sedimentary Petrology 1972; 42: 239- 242.

[28] Derrick MR, Strulik D, Landry JM. Infrared Spectroscopy in Conservation Science. Scientific Tools for Conservation. Getty Conservation Institute, USA; 1999, 235p.

[29] UNE-EN 1936. Métodos de ensayo para piedra natural: Determinación de la densidad real y aparente y de la porosidad abierta y total. Asociación Española de Normalización y Certificación (AENOR), Madrid, 2007.

[30] UNE-EN 14579. Métodos de ensayo de piedra natural. Determinación de la velocidad de propagación del sonido. Asociación Española de Normalización y Certificación (AENOR), Madrid, 2005.

[31] Dunham RJ, Classification of carbonate rocks according to depositional texture. In: Ham WE editor. Classification of carbonate rocks: American Association of Petroleum Geologists Memoir; 1962, p. 108-121.

[32] Fort R, Fernández-Revuelta B, Varas MJ, Álvarez de Buergo M, Taborda M. Influence of anisotropy on the durability of Madrid-region Cretaceous dolostone exposed to salt crystallization processes. Materiales de Construcción 2008; 58 (289-290): 161-178.

[33] Young ME, Cordiner P, Murray M. Chemical consolidants and water repellents for sandstones in Scotland. Edinburgh, Scotland Historic Scotland Research Report; 2003, 265 p.

[34] López-Arce P, Fort R, Gómez-Heras M, Pérez-Monserrat E, Varas-Muriel MJ. Preservation strategies for avoidance of salt crystallisation in El Paular Monastery cloister, Madrid, Spain. Environmental Earth Sciences 2011; 63 (7-8): 1487-1509.

[35] Varas MJ, Álvarez de Buergo M, Fort R. Natural cement as the procursor of Portland cement: methodology for its identification. Cement and Concrete Research 2005; 35(11): 2055-2065.

[36] Machel HG, Burton EA. Burial - diagenetic sabkha - like gypsum and anhydrite nodules. Sedimentary Geology 1991; 61: 394–405.

[37] Zamannejad A, Jahani D, Lotfpour M, Movahed B. Mixed evaporite/carbonate characteristics of the Triassic Kangan Formation, offshore area, Persian Gulf. Revista mexicana de Ciencias Geológicas 2013; 30 (3): 540-551.

FIGURE CAPTIONS

Fig. 1. Twelfth-thirteenth century Romanesque apse on church at Talamanca de Jarama, Madrid, Spain, whose upper stone ashlars are yellow and lower rough ashlars beige dolostone; occasional white limestone cladding

Fig. 2. Richly carved cornice and modillions on the upper part of the church, restored in 1990: cement mortar filling in inter-ashlar joints and laid directly on the cornice underneath the Spanish tile roof

Fig. 3. Decaying cornice and modillions in 2004, showing substantial amounts of cement on the cornice and the near total loss of ornaments on modillions and cornice

Fig. 4. Samples of dolostone on around the cornice: a) cross-section of yellow dolostone core: b) decayed fragment from cornice surface, showing the obvious contrast between the glossy grey treatments and the yellowish dolostone

Fig. 5. Grey treatment scaling and flaking on cornice and modillions, baring the yellow stone substrate and inducing the loss of the original restored ornament

Fig. 6. Cross-section of scale removed from cornice, showing three zones: upper grey layer with white particles and varying depth (restoration mortar), middle layer where the stone substrate exhibits cracks parallel to the surface and a few white spots, and lower layer where the yellow substrate is compact

Fig. 7. PM images of yellow dolostone on the upper part of the apse: a) no decay but substantial original porosity (left: parallel nicols; right: crossed nicols); and b) cracks and nodules indicative of decay (parallel nicols)

Table 1. Petrophysical properties of decayed (outer 5 cm) and undecayed (at depths of 5-10 cm) dolostone

Fig. 8. Scaling on cornice: a) PM image with parallel nicols; b) μXRD diffractogram showing the mineralogy of the two components of the restoration mortar; c) SEM-SE image of a thin section: A - restoration mortar, B – gypsum layer, C - cracked stone substrate with gypsum nodules

Fig. 9. SEM-SE image of a fragment of restoration mortar and EDS point chemical composition: A - binder; B – aggregate

Fig. 10. FTIR spectrum of restoration mortar

Fig. 11. Fragment of restoration mortar surface, showing: A - surface acrylic, B - binder and C - aggregate (both in the underlying restoration mortar), under: a) PM (parallel nicols) and b) SEM-SE. EDS point chemical composition of synthetic resins (A - acrylic and B - epoxy+acrylic) forming part of the two treatments (with Ca as the sole chemical element in the C - aggregate)

Fig. 12. FTIR spectrum of resin film

Fig. 13. SEM-SE image and EDS point chemical composition of a scaling fragment, showing: A - surface treatment, B - restoration mortar, C - gypsum layer and D - cracked stone substrate

Fig. 14. PM (parallel nicols) images of: a) gypsum nodules inside the cracked dolostone; and b) capillary connections.

Fig. 15. Mechanism governing post-1990 intervention decay in cornice and modillions: 1 - acrylic surface treatment; 2 - synthetic restoration mortar; 3 - gypsum layer; 4 - cracked dolostone with gypsum nodules; A - rainwater leakage; B - surface runoff.

Highlights

Long-term effectiveness, suitability and durability of conservation treatments

Need for preliminary studies to ensure successful restoration

Use of petrological techniques to determine treatment mechanisms

Unsuitable use of cements and synthetic resins on decayed dolostone

Salt-induced loss of restored ornaments

Fig. 1

Fig. 2

Fig. 3

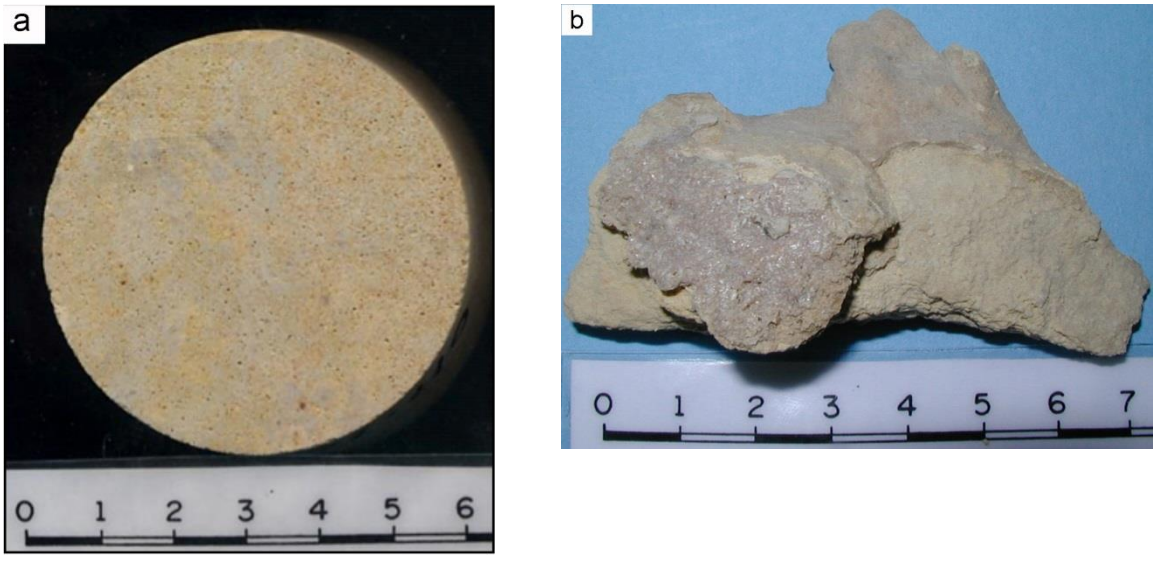

Fig. 4

Fig. 5

Fig. 6

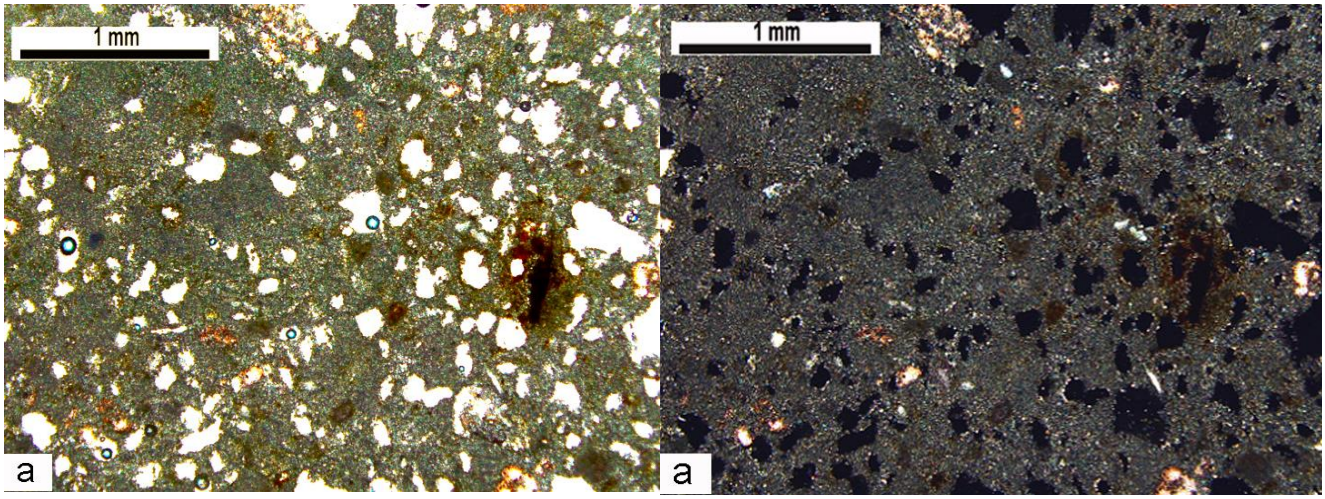

Fig. 7a

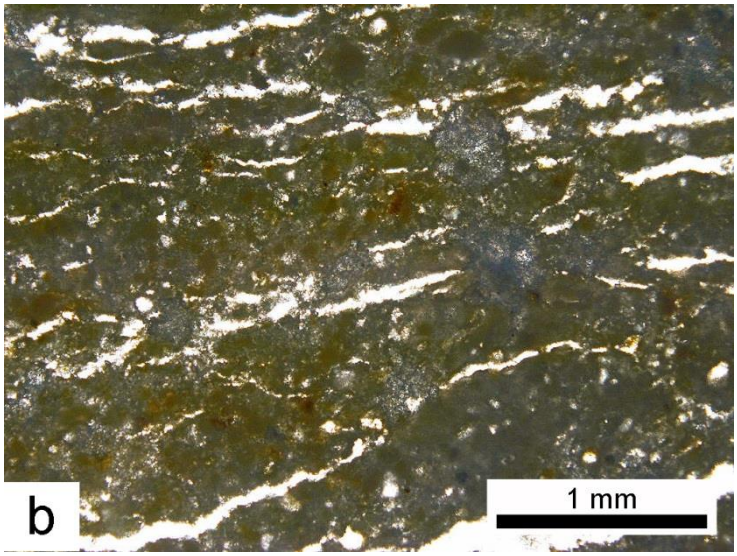

Fig. 7b

Table 1

	Dolostone	
	outer area	**inner area**
Real density (kg m^{-3})	2 821	2 824
Bulk density (kg m^{-3})	2 077	2 237
Open porosity (%)	26.36	24.31
Water absorption (%)	12.69	11.38
Vp (m s^{-1})	1 843	2 873

Vp - ultrasonic P-waves pulse velocity

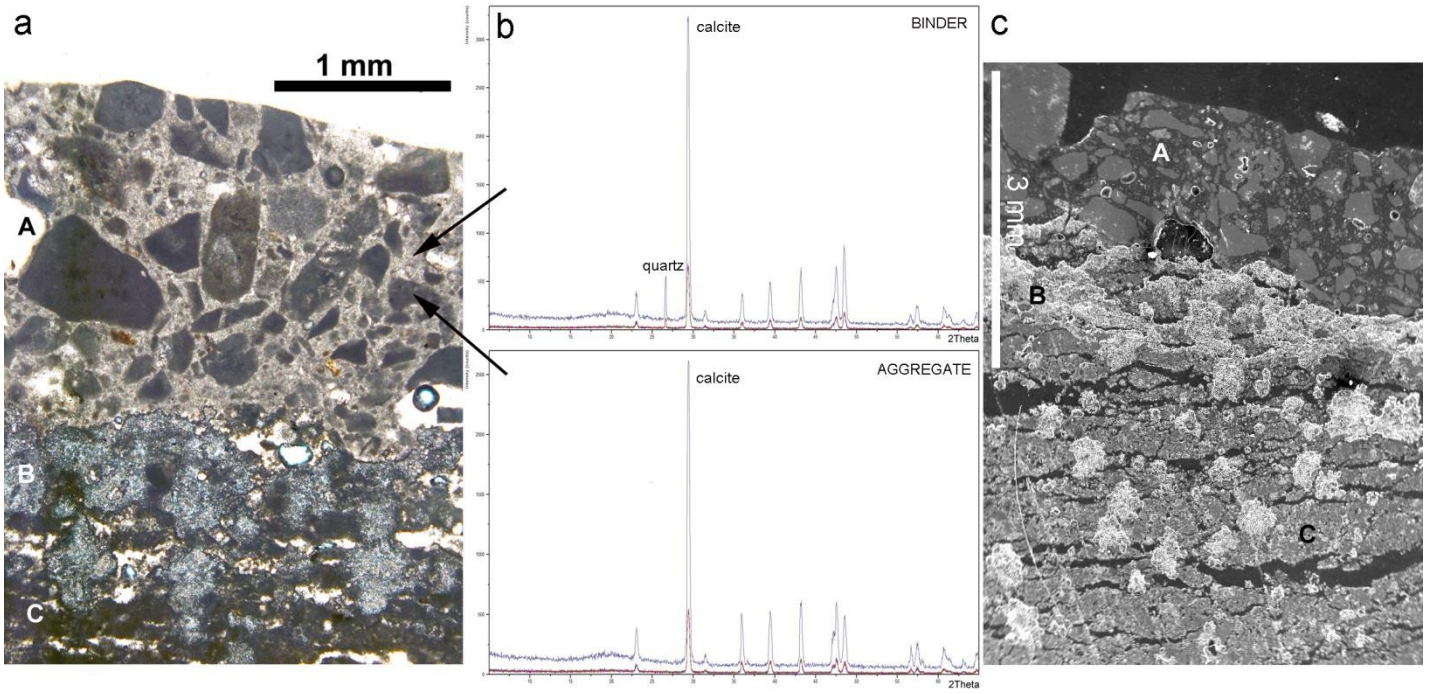
a
1 mm
A
B
C
b
calcite
BINDER
quartz
2Theta
calcite
AGGREGATE
2Theta
c
A
3 mm
B
C

Fig. 8

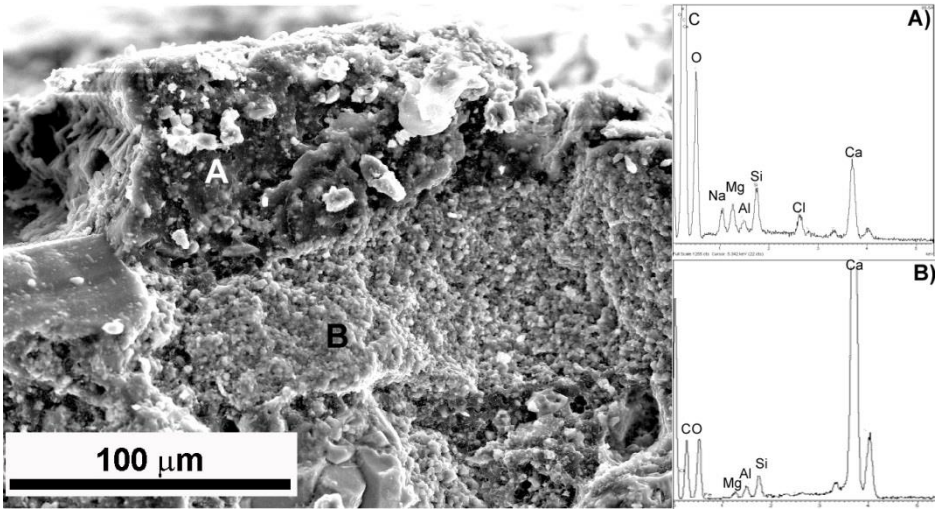
A
B
100 μm
C
O
Na
Mg
Al
Si
Cl
Ca
A)
Ca
B)
CO
Mg
Al
Si

Fig. 9

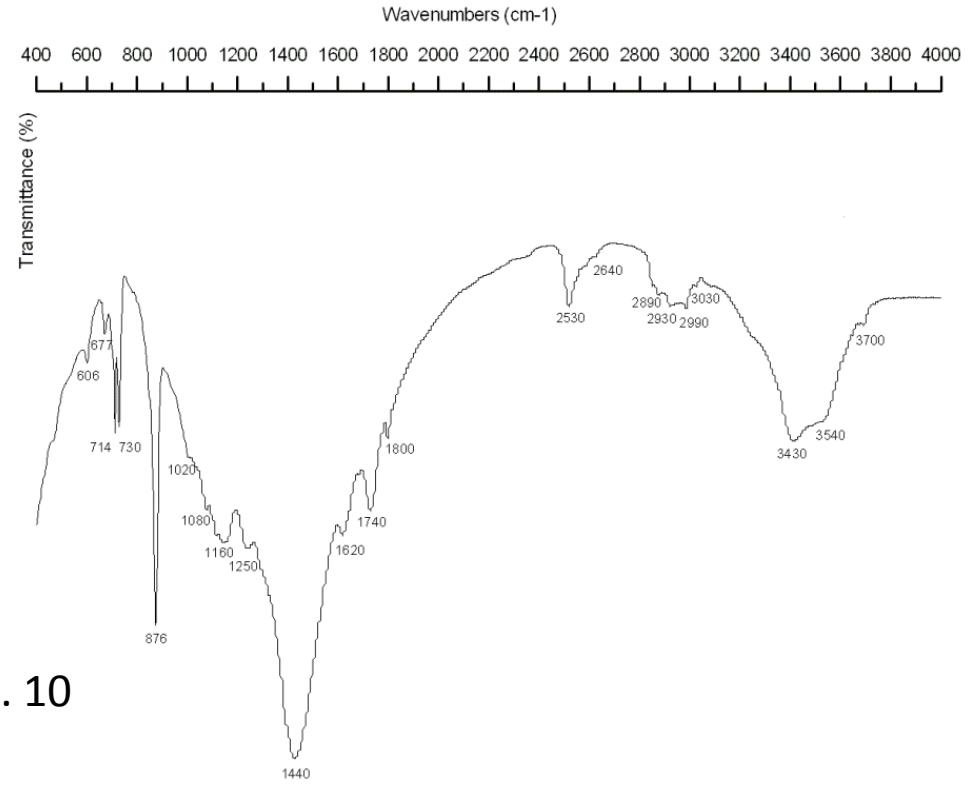
Wavenumbers (cm-1)
400 600 800 1000 1200 1400 1600 1800 2000 2200 2400 2600 2800 3000 3200 3400 3600 3800 4000
Transmittance (%)
606
677
714
730
876
1020
1080
1160
1250
1440
1620
1740
1800
2530
2640
2890
2930
2990
3030
3430
3540
3700

Fig. 10

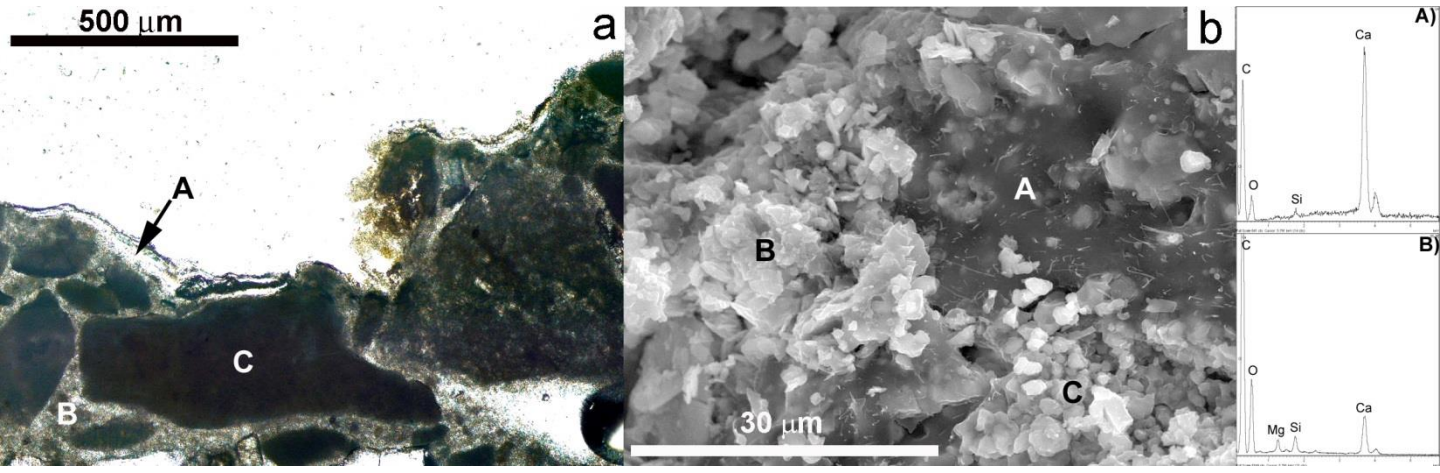
500 µm
a
A
C
B
b
A
B
C
30 µm
A)
Ca
C
O
Si
B)
C
O
Mg
Si
Ca

Fig. 11

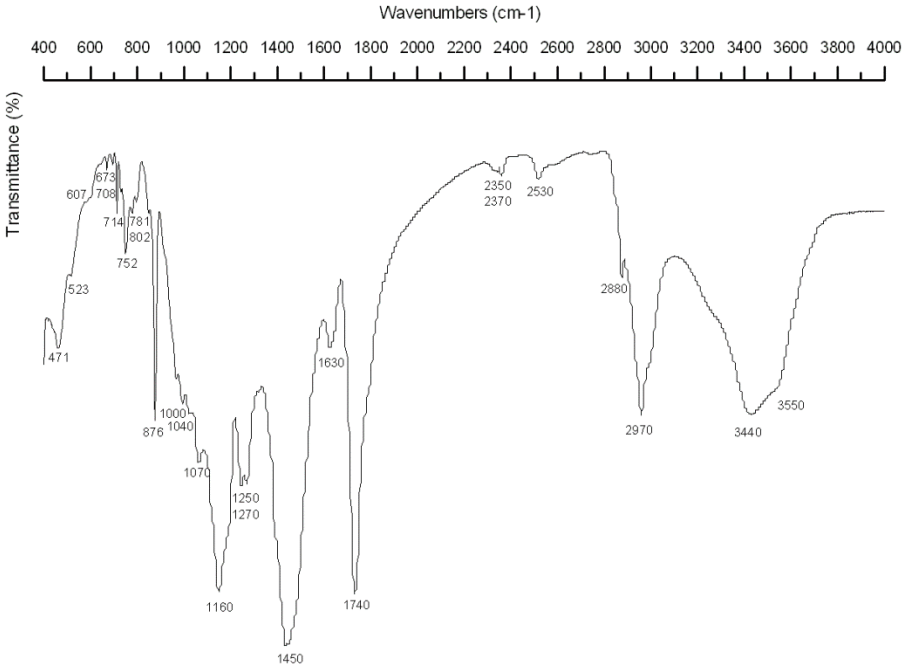
Wavenumbers (cm-1)
400 600 800 1000 1200 1400 1600 1800 2000 2200 2400 2600 2800 3000 3200 3400 3600 3800 4000
Transmittance (%)
607
673
708
714
781
802
752
523
471
876
1000
1040
1070
1160
1250
1270
1450
1630
1740
2350
2370
2530
2880
2970
3440
3550

Fig. 12

Fig. 13

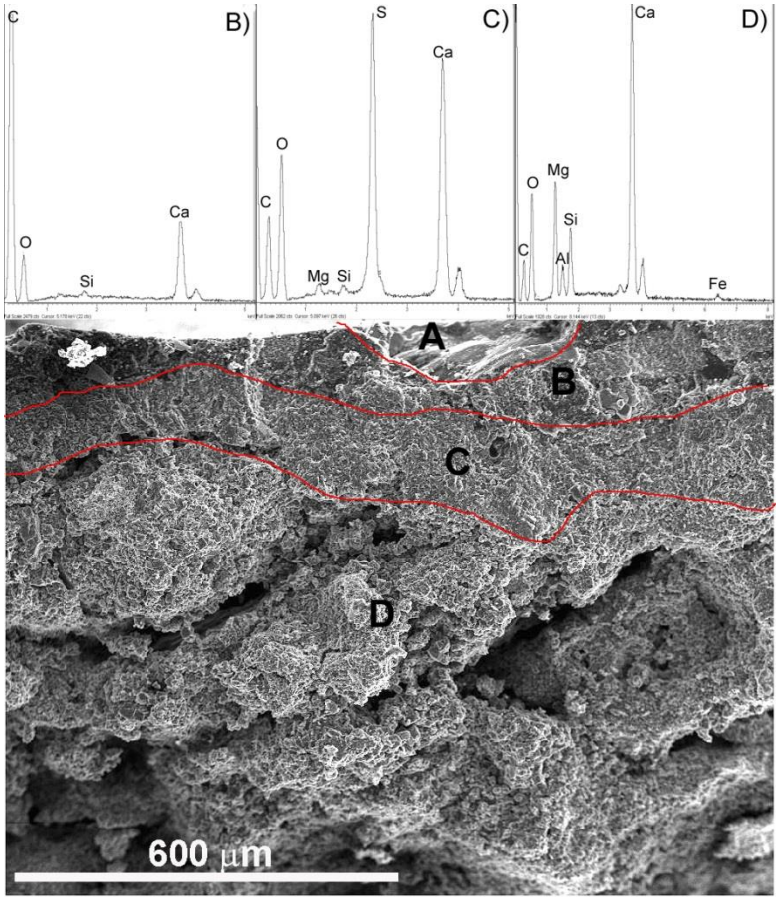
C
O
Si
Ca
B)
C
O
Mg
Si
S
Ca
C)
O
Mg
Si
C
Al
Ca
D)
Fe
A
B
C
D
600 µm

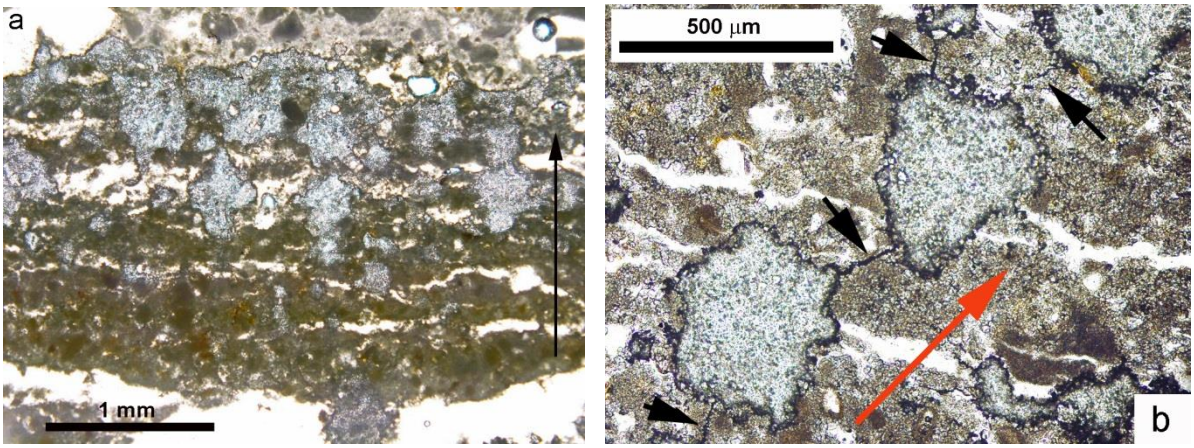

Fig. 14

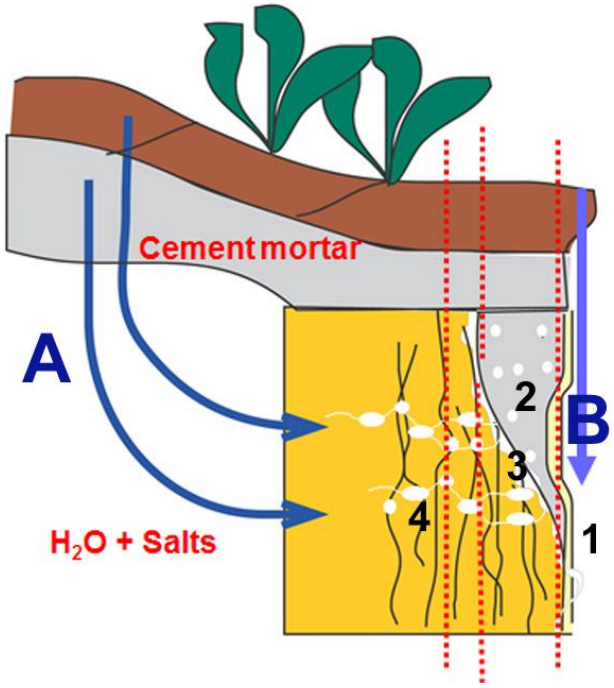

Fig. 15